Environmental Science and Pollution Research (2020) 27:37572–37580
https://doi.org/10.1007/s11356-020-09311-0

RESEARCH ARTICLE

Parameters and mechanism of membrane-oriented processes for the facilitated extraction and recovery of norfloxacin active compound

Rkia Louafy[1] · Abderezzak Benelyamani[2] · Sanae Tarhouchi[1] · Oussama Kamal[1] · Khalifa Touaj[1] · Miloudi Hlaibi[1,2]

Received: 28 March 2020 / Accepted: 13 May 2020 / Published online: 28 May 2020

Abstract

In the present work, a polymer inclusion membrane (PIM) using an amphiphilic molecule Tween 20 (TW20) as the carrier was developed and characterized to hinder environmental contamination caused by norfloxacin (NRF), an antibiotic widely used in veterinary and human medicines. Fourier-transform infrared spectroscopy (FTIR) and scanning electron microscopy (SEM) coupled with energy X-ray dispersion spectroscopy (EDS) were used to reveal the composition, porosity, and morphology of the elaborated membrane. In order to measure the performance of the as-developed membrane, the influences of NRF initial concentration (C_0 = 0.04 mol L^{-1}, 0.02 mol L^{-1}, 0.01 mol L^{-1}, and 0.005 mol L^{-1}), pH (2.6, 4.5, and 10.5), and temperature (T = 298 K, 303 K, and 305 K) were investigated. The evolution of macroscopic (permeability (P) and initial flux (J_0)), microscopic (association constant (K_{ass}) and apparent diffusion coefficient (D^*)), and activation parameters (activation energy (E_a), enthalpy ($\Delta H^{\neq}_{ass}$), and entropy ($\Delta S^{\neq}$)) was analyzed. It was found that TW20 was an effective agent for the extraction and recovery of different forms of NRF, especially the zwitterion form appeared at pH = 4.5. On the other hand, for the biologically active NRF compound, the mechanisms of the studied processes were controlled by the *kinetic aspect* rather than the *energetic* counterpart.

Keywords Polymer inclusion membranes · Oriented processes · Antibiotics · Permeability · Apparent diffusion coefficient · Kinetic and energetic aspects

Nomenclature

$[T]_0$	Concentration of carrier in the membrane phase (mol L^{-1})
C_0	Initial concentration of norfloxacin in the feed phase (mol L^{-1})
C_R	Concentration of norfloxacin in the receiving phase (mol L^{-1})
P	Permeability of the membrane (cm^2 s^{-1})
J_0	Initial flux (mmol s^{-1} cm^{-2})
D^*	Apparent diffusion coefficient (cm^2 s^{-1})
K_{ass}	Association constant
l	Membrane thickness (μm)
t	Time (s)
V	Volume of the receiving phase (cm^3)
S	Active area of the membrane (cm^2)
T	Temperature (K)
R	Ideal gas constant (J mol^{-1} K^{-1})
E_a	Activation energy (KJ mol^{-1})
$\Delta H^{\neq}_{ass}$	Activation association enthalpy (KJ mol^{-1})
$\Delta H^{\neq}_{diss}$	Activation dissociation enthalpy (KJ mol^{-1})
$\Delta S^{\neq}$	Activation entropy (KJ mol^{-1} K^{-1})

PPR2 Project: Ministry of Higher Education, Scientific Research and Management Training - National Center for Scientific and Technical Research

Responsible Editor: Tito Roberto Cadaval Jr

Electronic supplementary material The online version of this article (https://doi.org/10.1007/s11356-020-09311-0) contains supplementary material, which is available to authorized users.

✉ Miloudi Hlaibi
m.hlaibi58@gmail.com

[1] Laboratoire Génie des Matériaux pour Environnement et Valorisation (GeMEV), Faculté des Sciences Ain-Chock, Hassan II University of Casablanca (UH2C), B.P 5366 Maarif, Casablanca, Morocco

[2] Laboratoire de recherche et développement AFRIC-PHAR, Route régionale Casablanca/Mohammedia N° 322, Km 12, Aïn Harrouda, 28630 Casablanca, Morocco

Introduction

Pharmaceutical products pollute the aquatic ecosystem through several pathways, such as municipal wastewater, treatment plants, hospitals, pharmaceutical industries, and agricultural activities (Sim et al. 2011; Li et al. 2015a). Antibiotics are one the most widely prescribed therapeutic classes in human and veterinary medicines, and their intense use releases a large quantity of these active substrates into environmental waters (Martinez 2009; Chen and Zhou 2014; Hu et al. 2019a, b). Norfloxacin (NRF), a broad-spectrum fluoroquinolone antibiotic and one of the most commonly used drugs in human and veterinary medicines, is often found (ranks second among all fluoroquinolones) in drinking water and wastewater (Wang et al. 2018). Haiyang Chen et al. (2018) investigated the risks of thirteen different types of antibiotics to the aquatic environment of the Hai River system (HRS) in China and detected the presence of NRF in 228 samples with a frequency rate of 80.4%.

Membrane-oriented processes are one of the most effective techniques to impede the problems of environmental contamination (Taheran et al. 2016; Kamrani et al. 2018; Chaouqi et al., 2019a, b). Membrane technology is considered an alternative or complementary separation process for conventional treatment techniques, such as liquid-liquid extraction, distillation, and adsorption (C.J.M. van Rijn 2004). The development of affinity membranes is still under progress; thus, their industrial applications are very limited. These biological membranes are composed of lipid bilayers in which amphipathic molecules act as specifically designed receptors and allow communications between cells by controlling their selective permeability (Watson 2015). Polymer membranes are generally functionalized with selective carriers (extractive agents) consisting of different functional groups, such as –OH, –COOH, –NH2, and –SH (Lewis et al. 2012; Chaouqi et al., 2019a, b; Demire and Gerbaud 2019). Polymer inclusion membranes (PIMs) mainly consist of a polymer support and a carrier, which reacts reversibly with the permeant and which can act in some cases as a plasticizer and in other cases by incorporating a plasticizer or modifier to provide flexibility and high mechanical stability of membranes (Spas, 2019). PIMs are an attractive alternative to supported liquid membranes (SLMs), which are known for their instability due to the loss of solvents, and therefore of the membrane phase carrier, thus decreasing their lifetime and then limiting their application (Hao et al. 2017; Spas, 2019).

Polysorbates or Tweens are nonionic surfactants in which fatty acid esters are attached as a tail to polyethoxysorbitan (head group). Tweens 20, 40, 60, 65, and 80 are widely used in the food and cosmetic products and biopharmaceutical formulations to protect and stabilize proteins (Wang et al. 2019; Hu et al., 2019a, b). In the present work, Tween 20 (TW20) was integrated to the membrane phase as the carrier (Fig. S1a), because it is an amphiphilic molecule and can attach to the polymer phase through the hydrophobic part; hence, the hydrophilic part with functional groups is oriented outwards to associate with the substrate to be extracted.

A PIM affinity polymer membrane using TW20 as the carrier was developed and characterized for the extraction and recovery of NRF compound (Fig. S1b) from an aqueous solution, whose the main objective is the treatment of pharmaceutical effluents for the contribution of the environmental protection. In order to measure the performance of the as-developed membrane, the influences of NRF initial concentration (C_0), pH, and temperature (T) on the evolution of macroscopic (permeability (P) and initial flux (J_0)), microscopic (association constant (K_{ass}) and apparent diffusion coefficient (D^*)), and activation (activation energy (E_a), enthalpy ($\Delta H^{\neq}_{ass}$), and entropy ($\Delta S^{\neq}$)) parameters were analyzed.

Methods, chemicals, and materials

The membrane was prepared by dissolving polyvinylidene fluoride PVDF (2 g; MW = 35,000; purchased from HIMEDIA) in N,N-dimethyl formamide (DMF; 12 mL; 99.8%; purchased from Sigma-Aldrich) at 60 °C, and then an equivalent mass of 0.5×10^{-3} mol of TW20 (polysorbate 20; $d = 1.1$ g cm^{-3}; FW = 1228 g mol^{-1}; purchased from Merck KGaA) was added as a carrier molecule. After dissolution, 2-nitrophenyl octyl ether NPOE (100 μL; ≥ 99%; d = 1.04 g cm^{-3}; purchased from Fluka) was added as a plasticizer, and the mixture was stirred for 72 h. After the total insertion of the carrier, the obtained polymer solution was spread uniformly on the surface of a glass plate by a ruler, then kept in air for 30 s, and subsequently put in an oven for 12 min to allow the evaporation of the solvent. Further, the plate was immersed in distilled water as non-solvent coagulation bath (conductivity ≤ 2 μS cm^{-1}) at room temperature. The thickness (l = 137 μm) of the obtained membrane was measured by an electronic micrometer (Mitutoyo) at 12 different points along the cut edge, and the concentration of the inserted carrier in the membrane phase was calculated as $[T]_0$ = 0.171 mol L^{-1}.

Scanning electron microscopy coupled with energy X-ray dispersion spectroscopy (SEM-EDS; ZEISS EVO40 EP) was employed to determine the morphology and elemental composition of the as-prepared membranes (PVDF support and PVDF/TW20/NPOE). Before the analysis, the membranes were coated with gold spray, and for cross-section, liquid nitrogen was used to freeze the membranes before the fractures. A Fourier-transform infrared spectrometer (FTIR; FT/IR–4600) equipped with an attenuated total reflectance (ATR) accessory (Pro one) was used to identify the composition of the prepared membrane and to justify the presence of the

carrier in the polymer matrix at a resolution of 4 cm^{-1} over the spectral range 4000–300 cm^{-1}.

The transport cell consisted of two glass compartments, which were separated by the membrane (M) with an active contact surface (S) of 10.75 cm^2. The feed compartment (F) contained the NRF (FW = 319, 33; purchased from Alfa Aesar; initial concentration (C_0) ranged from 4×10^{-2} mol L^{-1} to 5×10^{-3} mol L^{-1}), and the receiving compartment (R) contained distilled water adjusted to the same pH of the feed solution. The system was immersed in a water-containing thermostatic bath to maintain the same temperature during the extraction process (Fig. S2). The pH of the medium was measured by a titrator (Easy Pro, Mettler Toledo) at 2.6 and 4.2 (acidified with 1 mol L^{-1} HCl; 37%; purchased from Sigma-Aldrich) and at 10.5 (adjusted with 1 mol L^{-1} NaOH; FW = 40, 99.1%, purchased from VWR).

The evolution of the extracted NRF substrate concentration with time was analyzed at the maximum absorption wavelength (λmax = 277 nm) from the receiving phase by a UV-Vis spectrophotometer (UV/VIS Excellence, Mettler Toledo) in the wavelength range of 190–1100 nm.

Theoretical models

Numerous studies have been carried out to analyze the performance of affinity membranes (Eljaddi et al. 2015; Kamal et al. 2017; El Atmani et al. 2018). These studies have elucidated two theoretical models to quantify the studied process:

– The kinetic model (MS1) based on the first Fick's law determines macroscopic parameters (P and J_0).

$$\mathbf{P} \times (\mathbf{t}-\mathbf{t_l}) = \left(\mathbf{l} \times \frac{\mathbf{V}}{\mathbf{S}}\right)\left(\frac{1}{2} \times \mathbf{Ln}\left(\frac{\mathbf{C_0}}{\mathbf{C_0}-2\mathbf{C_R}}\right)\right) \quad (1)$$

$$\mathbf{P} = \frac{\mathbf{a} \times \mathbf{V} \times \mathbf{l}}{2\mathbf{S}} \quad (2)$$

$$J_0 = \frac{P \times C_0}{l} \quad (3)$$

With: l = membrane thickness, S = membrane active area, V = receiving phase volume, C_0 = initial substrate concentration in the feed phase, and C_R = substrate concentration in the receiving phase at time t.

– The thermodynamic model (SM2) based on the second Fick's law (according to the saturation law of the agent T by the substrate S (Michaelis-Menten type)) calculates microscopic parameters (K_{ass} and D^*) and established the relationship between J_0 and C_0.

$$1/\boldsymbol{J}_0 = \left(\boldsymbol{l}/\boldsymbol{D}^*\right) \times \left[\left(1/\left([\mathbf{T}]_0 \times \boldsymbol{K_{ass}}\right)\right) \times \left(1/\mathbf{C}_0\right) + \left(1/[\mathbf{T}]_0\right)\right] \quad (4)$$

The slopes (p) and intercepts (OO) of line segments relating to the Lineweaver-Burk representation ($1/J_0 = f\,(1/C_0)$) determine the values of K_{ass} and D^*.

$$K_{ass} = \frac{\text{intercept } (oo)}{\text{slope } (p)}; D^* = \left(\frac{1}{\text{oo} \times [T]_0}\right) \quad (5)$$

The initial flux J_0 evolves with temperature according to the Arrhenius relationship (Xu et al., 2007).

$$J_0(T) = A_j \times e^{\left(\frac{-E_a}{RT}\right)} \quad (6)$$

With: R = ideal gas constant (8.314 J mol^{-1} K^{-1}) and A_j = pre-exponential term proportional to the number of favorable interactions between the substrate and the carrier.

The slope (p) and intercept (OO) of the linear function in Eq. 7 determine the values of E_a and A_j and then calculate $\Delta H^{\#}$ and $\Delta S^{\#}$ at 298 K according to the theory of transition states (Eyring theory) (Eqs. 8 and 9):

$$\mathbf{LnJ}_0 = -\left(\frac{\mathbf{E_a}}{\mathbf{R}}\right) \times \left(\frac{1}{\mathbf{T}}\right) + \mathbf{LnA_j} \quad (7)$$

$$\Delta\mathbf{H}^{\neq} = \mathbf{E_a} - 2500 \quad (8)$$

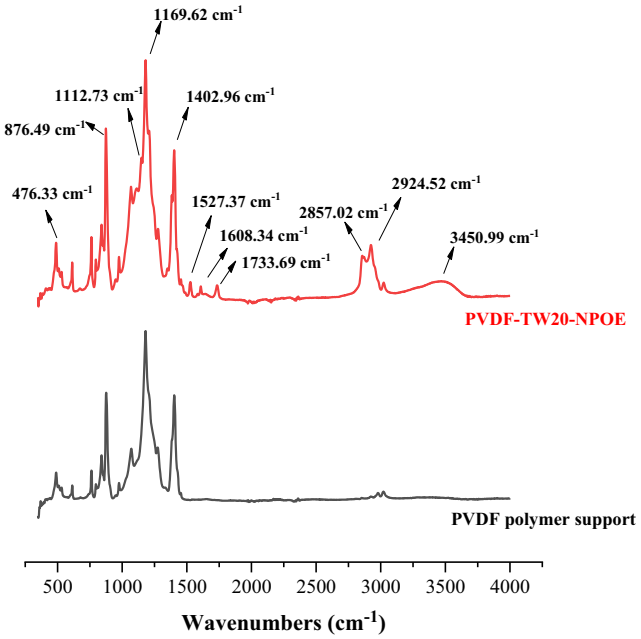

Fig. 1 FTIR spectra of PVDF polymer support and PVDF-TW20-NPOE developed membrane

$$\Delta S^{\neq} = R \times \left(\mathrm{LnA_j} - 30.46\right) \quad (9)$$

The variation of K_{ass} (equilibrium constant of the association-dissociation reaction) as a function of temperature determines the thermodynamic enthalpy ΔH_{th} according to the isobaric Van't Hoff equation.

$$\frac{d\mathrm{Ln}K_{ass}}{dT} = \frac{\Delta H_{th}}{RT^2} \quad (10)$$

with a $= \frac{\Delta H_{th}}{R}$ $a = \Delta H_{th}/R$ is the slope of the linear function.

$$\mathrm{Ln}K_{ass} = f\left(\frac{1}{T}\right) \quad (11)$$

ΔH_{th} is related to the association ($\Delta H^{\neq}_{ass}$) and dissociation ($\Delta H^{\neq}_{dis}$) energies (activation parameters relating to the transition state) according to the following expression.

$$\Delta H^{\neq}_{th} = \Delta H^{\neq}_{ass} - \Delta H^{\neq}_{diss} \quad (12)$$

The $\Delta H^{\neq}_{dis}$ parameter is determined to confirm the nature of the aspect (energetic or kinetic), which controls the oriented process through an elaborated PIM.

Results and discussion

Characterization of the membranes

After the preparation of the membrane, studies on their composition and morphology were performed. The FTIR spectra of the as-prepared membranes are presented in Fig. 1. The peaks existing in the range of 470–1400 cm^{-1} correspond to PVDF fingerprints, and the presence of the new absorption bands at 3450.99 cm^{-1} and 1733.69 cm^{-1} appeared due to

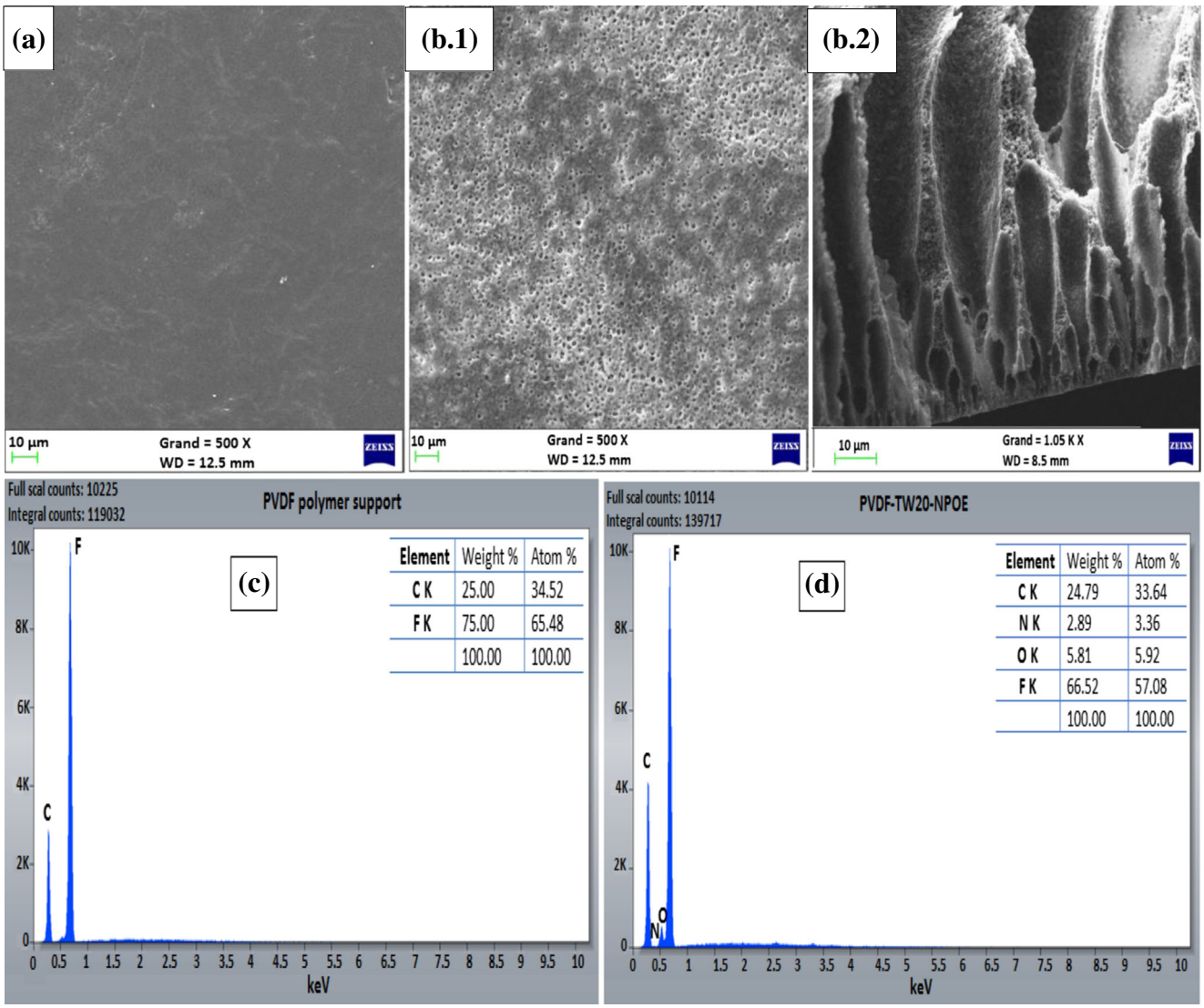

Fig. 2 SEM images of polymer support PVDF surface (**a**) and PVDF/TW20/NPOE membrane surface (**b1**) and cross section (**b2**) and their EDS spectra (**c** and **d**)

Table 1 Evolution of P and J_0 parameter values, depending on the NRF initial concentration C_0

C_0 (mol L^{-1})	$P.10^7$ (cm^2 s^{-1})	$J_0.10^5$ (mmol s^{-1} cm^{-2})
0.04	17.812	0.552
0.02	18.209	0.282
0.01	18.431	0.143
0.005	19.153	0.074

the stretching vibration of O–H alcohol and C=O ester groups, respectively. The appearance of the weak peak at 1112.79 cm^{-1} was generated due to the stretching vibration of the C–O–C ether group. The doublets at 2857.02 cm^{-1} and 2924.52 cm^{-1} appeared from the symmetric and asymmetric stretching vibration of CH_2, and an increase in their intensities indicates that their concentrations increased after the addition of TW20 in the membrane phase.

The SEM-EDS images of surfaces and cross sections of the membranes (Fig. 2) reveal a clear difference in their porosity. The top surface of the PVDF support membrane had a dense skin layer without pores (Fig. 2a), and after the integration of TW20 agent, the porosity of the PVDF support membrane increased (Fig. 2b1). The cross section of the PVDF/TW20/NPOE membrane is presented in Fig. 2b2, and it is clear that it possessed an asymmetric structure consisting of finger-like porous support. The EDS spectra show the elementary composition of two membranes. In the PVDF support membrane, only a high percentage of carbon and fluorine was detected (Fig. 2c), and the appearance of oxygen signal at around 0.5 keV (Fig. 2d) confirms the presence of the carrier in the membrane phase, which is already proven by FTIR analysis.

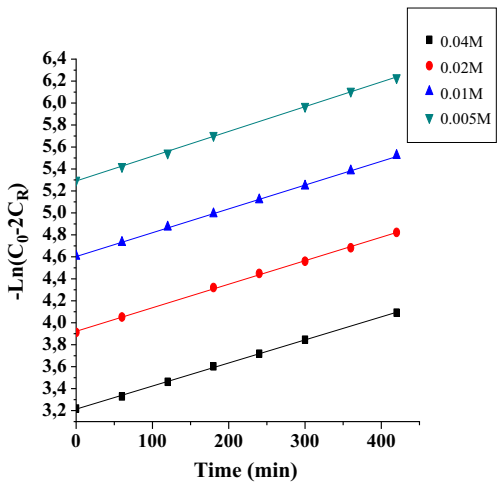

Fig. 3 Kinetic model verification (–Ln (C_0–$2C_R$) = $f(t)$) for the studied processes at different initial concentrations of NRF substrate (pH = 4.5 and T = 298 K)

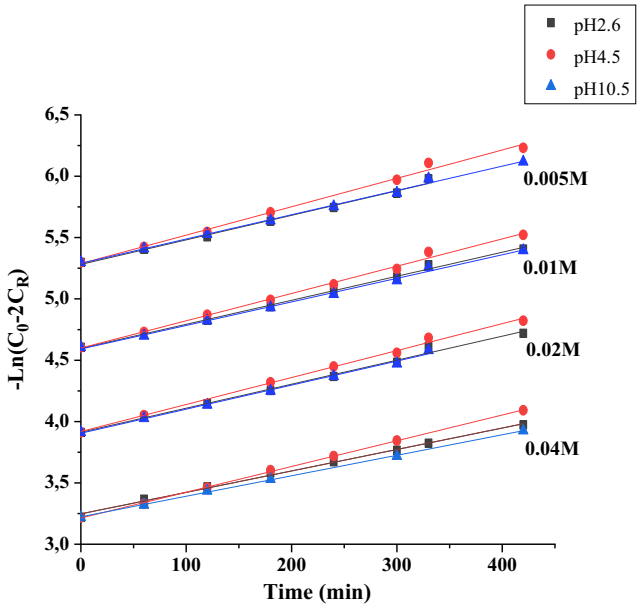

Fig. 4 Influence of acidity factor on the evolution of the kinetic function –Ln (C_0–$2C_R$) = $f(t)$), at different pH (2.6, 4.5, and 10.5), different concentrations C_0 (0.04, 0.02, 0.01, and 0.005 mol L^{-1}), and at T = 298 K

Quantification of the studied oriented processes

Influences of NRF substrate initial concentration

The influences of NRF initial concentration (C_0) on the evolution of P and J_0 parameters were investigated at pH = 4.5 and T = 298 K (Table 1). These parameters were determined from the representation of the kinetic function –Ln (C_0–$2C_R$) = $f(t)$ $-\mathrm{Ln}(C_0 - 2C_R) = f(t)$ (Eq. 1) presented in Fig. 3. The linear evolution of the kinetic function indicates that the facilitated extraction processes results of NRF substrate through the elaborated PIM are well adapted to the developed

Table 2 Acidity influence on the evolution of P and J_0 parameters for the extraction oriented processes across elaborated membrane

pH	C_0 (mol L^{-1})	$P.10^7$ (cm^2 s^{-1})	$J_0.10^5$ (mmol s^{-1} cm^{-2})
2.6	0.04	14.254	0.442
	0.02	15.962	0.247
	0.01	16.093	0.125
	0.005	16.408	0.064
4.5	0.04	17.837	0.553
	0.02	18.209	0.282
	0.01	18.431	0.143
	0.005	19.153	0.074
10.5	0.04	14.200	0.440
	0.02	15.782	0.245
	0.01	16.097	0.125
	0.005	16.389	0.064

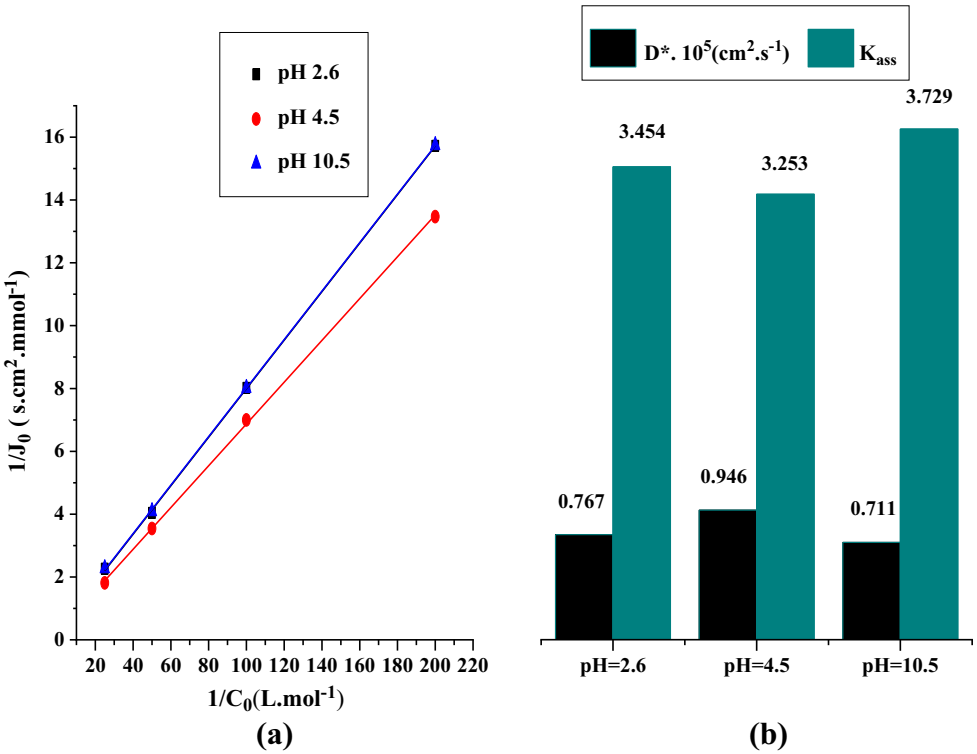

Fig. 5 Lineweaver-Burk presentations $1/J_0 = f(1/C_0)$ for facilitated extraction processes of NRF substrate (**a**). Evolution of K_{ass} and D^* parameters for studied oriented processes (**b**)

kinetic model, with the diffusion of NRF molecules through the membrane which is a rate-determining step.

The slopes of the straight lines in Fig. 3 were used to calculate permeability (***P***) (Eq. 2), which makes it possible to calculate the corresponding initial flux (J_0) (Eq. 3). The obtained results presented in Table 1 indicate that the membrane permeability increased with the decrease of NRF initial concentration C_0 and conversely of J_0. Indeed, this evolution is certainly due to the particular mechanism of the processes carried out.

Influences of the acidity factor (pH)

The acidity factors (pH) of feeding and receiving aqueous solutions had a significant effect on the facilitated extraction processes of NRF through the elaborated PIM membrane.

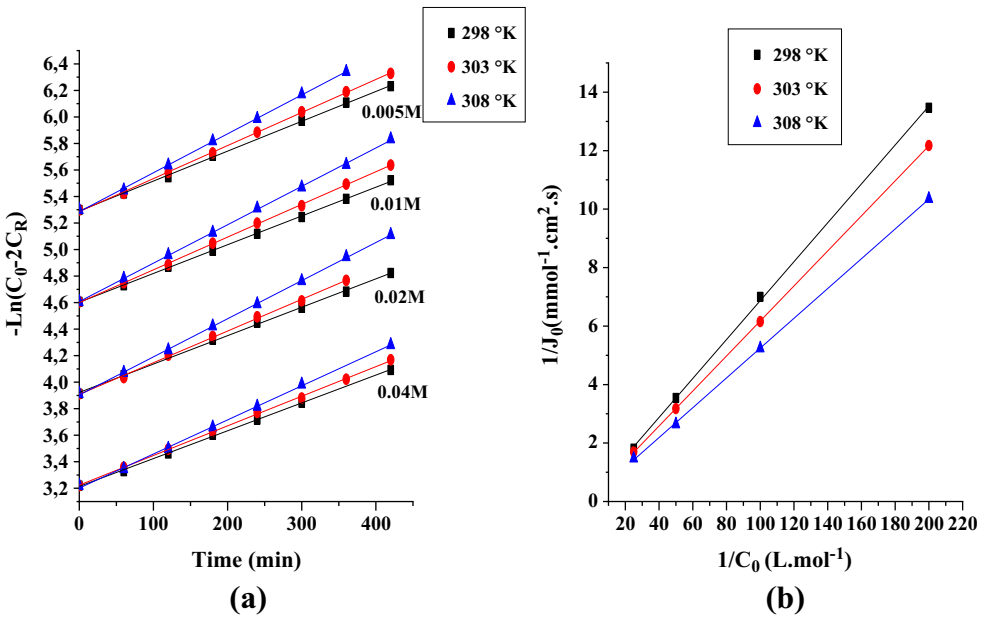

Fig. 6 The kinetic function presentation (**a**) and the Lineweaver-Burk presentation (**b**) for the extraction processes of NRF substrate at three studied temperatures

Table 3 Influence of temperature factor on the evolution of macroscopic and microscopic parameters P, J_0, D^*, and K_{ass}

T (K)	$P.10^7$ (cm^2 s^{-1})	$J_0.10^5$ (mmol s^{-1} cm^{-2})	$D.10^5$ (cm^2 s^{-1})	K_{ass}
298	18.408	0.263	0.946	3.253
303	20.358	0.287	1.104	3.094
308	23.949	0.336	1.363	2.947

NRF molecule is composed of carboxylic and amine groups, characterized successively by their acidity constants $pKa_1 = 5.58$ and $pKa_2 = 8.68$, respectively. Hence, depending on the pH of the aqueous solution, NRF molecules can exist in cationic, zwitterionic, or anionic forms (Roland Barret 2018). In order to examine the influences of pH on the evolution of P and J_0, experiments were carried out at three different pH values (2.6, 4.5, and 10.5) for different initial concentrations (C_0) and $T = 298$ K (Fig. 4). As norfloxacin is insoluble in a purely neutral medium under our work conditions, the pH value was selected as 4.5.

The different straight lines in the graph of Fig. 4 present the linear evolution with correlation coefficients (R^2) greater than or equal to 0.99 for all standardized experimental conditions. The slope values of these segments were used to calculate the values of P and J_0 parameters, and Table 2 summarizes the obtained results for different pH values.

Data in Table 2 clearly indicate that the elaborated membrane was more efficient at the intermediate acidity (pH = 4.5). Therefore, the zwitterionic form of the NRF substrate diffused more rapidly through the PVDF-TW20 PIM membrane than its cationic and anionic counterparts. In order to confirm this result, it is necessary to calculate the microscopic parameters, the association constant (K_{ass}) relating to the interaction of the substrate with the carrier to form unstable entities (ST), and the apparent diffusion coefficient (D^*) relating to the movement nature of NRF substrate molecules through the membrane phase. The thermodynamic model based on Fick's second law and the saturation law of the carrier by the substrate (Michaelis-Menten type) was used to establish the relationship between J_0 and C_0 according to the expression in Eq. 4. The values of K_{ass} and D^* specific parameters were determined from the slopes (p) and intercepts (OO) of the line segments presented in Fig. 5b according to the Lineweaver-Burk presentation $1/J_0 = f(1/C_0)$ (Fig. 5a).

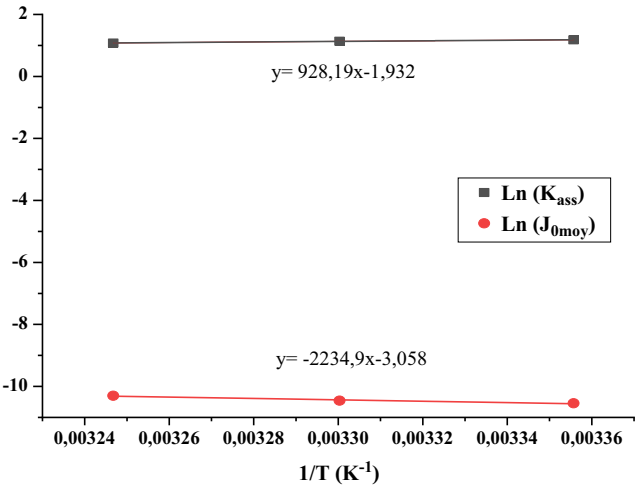

Fig. 7 Linear evolution for the presentations of Arrhenius and Van't Hoff relationships

Analysis of obtained results shows that the thermodynamic model is well verified, indicates an opposite evolution of D^* and K_{ass}, and confirms that the diffusion of the substrate through the membrane was conditioned by successive interactions of substrate molecules with *semi-mobile interaction sites* of the immobilized carrier in the membrane phase. When D^* was high, K_{ass} was weak; it signifies that for weak interactions of the substrate with the carrier (unstable ST), the membrane was more efficient for the studied processes. On the contrary, the best extraction of the zwitterion form was achieved at the pH values between two pKa values of NRF molecules because two opposite charges ensured an easy association and dissociation of this form with the carrier.

All these observations make it possible to envisage for the studied processes, a *mechanism by successive jumps* of NRF substrate molecules from one site to another of the immobilized carrier in the membrane phase. However, an examination of the temperature factor influence is necessary in order to confirm this mechanism and to elucidate the *energetic or kinetic* aspect that controls the oriented membrane processes related to the extraction and recovery of the NRF compound.

Influences of the temperature factor

In order to examine the effects of temperature on the membrane performance towards the NRF substrate studied, experiments were performed at three different temperatures (298 K, 303 K, and 308 K) and pH = 4.5 (acidity medium where the membrane is more efficient). The slopes of the line segments in Fig. 6a (obtained by the representation of the kinetic function $-\mathrm{Ln}(C_0 - 2C_R) = f(t)$) were used to calculate the values of P and J_0, and the Lineweaver-Burk presentation $1/J_0 = f(1/C_0)$ (Fig. 6b) allowed us to determine the values of D^* and K_{ass} parameters according to the expressions in Eq. 5. The obtained results are presented in Table 3.

Table 4 Evolution of activation and thermodynamic parameters for the facilitated extraction processes of NRF through the PIMs

E_a (KJ mol^{-1})	$\Delta H^{\neq}_{ass}$ (KJ mol^{-1})	$\Delta S^{\neq}$ (KJ mol^{-1} K^{-1})	ΔH_{th} (KJ mol^{-1})	$\Delta H^{\neq}_{dis}$ (KJ mol^{-1})
18.578	16.101	− 0.279	− 7.717	23.818

Data in Table 3 summarizes all results which indicate that the temperature factor had a profound effect on the evolution of the studied parameters. The values of P, J_0 and D^* parameters are increased with the increase of the temperature, and consequently, the membrane became more efficient. However, the decrease of K_{ass} with the increasing temperature indicates that the ST entity became unstable with the easy dissociation and faster diffusion of NRF molecules through the membrane phase, governed by the path of the substrate from one semi-mobile site to another of the fixed carrier, which results in a *double vehicle and jump mechanism on semi-mobile sites*, often translating the extraction oriented processes through PIM members (Li et al., 2015b). On the contrary, the value of K_{ass} did not vary greatly with the change of the temperature; hence, it can be inferred that the mechanism of these studied oriented processes were *controlled by a kinetic aspect*. In order to explain these results and confirm the mechanism type and the aspect that controls these oriented processes, activation and thermodynamic parameters have been calculated from the Arrhenius and Van't Hoff relationships presented by the functions Ln ($J_{0\ moy}$) = f (1/T) and Ln (K_{ass}) = f (1/T), respectively (Eqs. 7 and 11, respectively) (Fig. 7).

The straight segments in Fig. 7 present the evolution of the functions Ln ($J_{0\ moy}$) and Ln (K_{ass}) with the factor (1/T). The slopes and the intercepts of these line segments were used to calculate activation and thermodynamic parameters according to Eqs. 8, 9, and 12, and the corresponding results are presented in Table 4.

For activation and thermodynamic parameters (Table 4), the low values obtained during the association of the NRF substrate with TW20 carrier in the membrane phase (transition state) allowed to form an unstable entity (ST), thus leading to a high performance of the developed membrane. The negative value of activation entropy ($\Delta S^{\neq}$) indicates that the transition state is order and required little energy, so this is an *early state* and was easily formed. The relatively low value of activation enthalpy ($\Delta H^{\neq}_{dis}$) corresponding to the easy dissociation of the ST entity (Fig. 8) allowed a weak passage for NRF substrate molecules from one semi-mobile site to another of the fixed carrier during its movement through the membrane phase. The value $\Delta H^{\neq}_{dis}$ confirms that the studied oriented processes for the facilitated extraction of NRF compound through the elaborated PIM membrane were governed by the structural aspect (*kinetic control*) rather than the energetic aspect (*energetic control*).

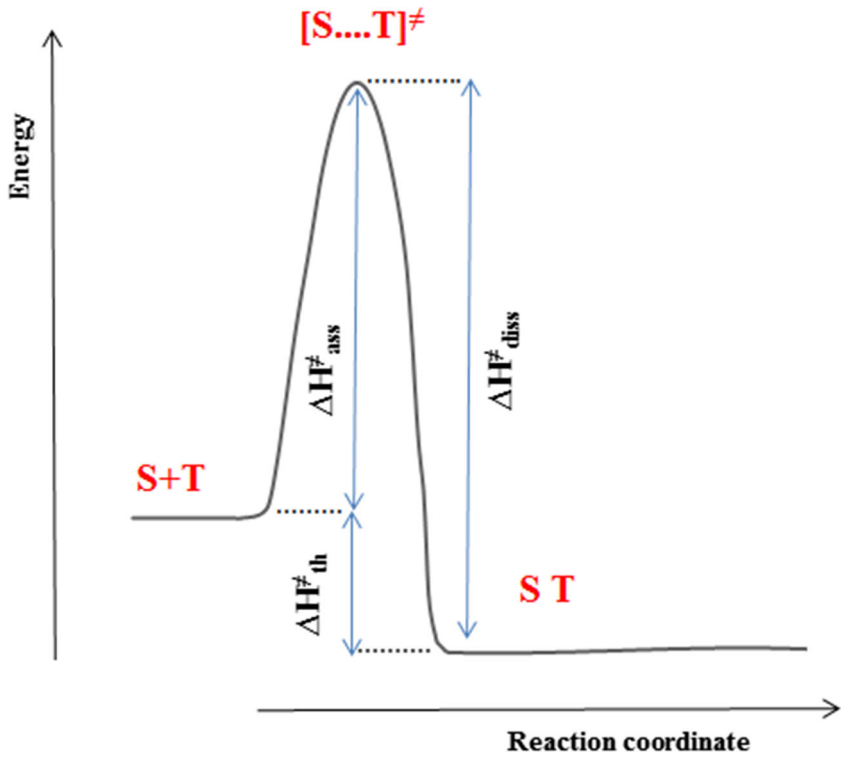

Fig. 8 Description of energetic diagram for the diffusion movement of the NRF substrate through the membrane phase (kinetically determining step of the mechanism)

Conclusion

In the present work, a PIM affinity polymer membrane using an amphiphilic molecule (TW20) as the carrier was developed by the phase inversion method for the extraction and recovery of the NRF compound. The influences of NRF initial concentration, pH, and temperature on the performance of the as-developed membrane were investigated, and the evolution of macroscopic, microscopic, and activation parameters relating to the facilitated extraction processes of NRF substrate was analyzed. The values of K_{ass} and D^* specific parameters indicate the nature of interactions between substrate molecules and semi-mobile sites of TW20 carrier, whereas values of $\Delta H^{\neq}_{ass}$ and $\Delta H^{\neq}_{dis}$ expresse that for the biologically active NRF compound, the mechanisms of studied processes were controlled by *kinetic aspect* rather than *energetic* counterpart. This is an important result which indicates that all mechanisms of oriented processes relating to the diffusion of compounds with biological or pharmaceutical activities through the affinity polymer membranes are controlled *by kinetic structural aspects* and not by energetic aspect and perform well at low temperatures. It was found that TW20 was an effective agent for the extraction and recovery of different forms of NRF, especially the zwitterion form appeared at pH = 4.5.

Funding information This work was financially supported by the Ministry of Higher Education and Scientific Research (MESRSFC) Morocco and the National Center for Scientific and Technical Research (CNRST) Morocco, out within the framework of the PPR2 project.

References

Roland Barret (2018) *Principes fondamentaux de chimie thérapeutique: Médicaments, propriétés physico-chimiques, prodrogues, pharmacophore*

Chaouqi Y et al (2019a) Oriented processes for extraction and recovery of blue P3R dye across hybrid polymer membranes: parameters and mechanism. *J Membrane Sci Res* 5:303–309. https://doi.org/10.22079/JMSR.2019.97857.1229

Chaouqi Y et al (2019b) Polymer inclusion membranes for selective extraction and recovery of hexavalent chromium ions from mixtures containing industrial blue P3R dye. Ind Eng Chem Res 58:18798–18809. https://doi.org/10.1021/acs.iecr.9b03026

Chen K. and Zhou J. L. (2014) Occurrence and behavior of antibiotics in water and sediments from the Huangpu River, Shanghai, China. *Chemosphere*. Elsevier Ltd.604–612. https://doi.org/10.1016/j.chemosphere.2013.09.119

Chen H. *et al.* (2018) Characterization of antibiotics in a large-scale river system of China: occurrence pattern, spatiotemporal distribution and environmental risks. *Science of the Total Environment*. Elsevier B.V.409–418. https://doi.org/10.1016/j.scitotenv.2017.11.054

Yaşar Demire; Vincent Gerbaud (2019) MEMBRANE TRANSPORT.in *Nonequilibrium Thermodynamics*.453–487. https://doi.org/10.1016/B978-0-444-64112-0.00010-1

El Atmani E. H. *et al.* (2018) The oriented processes for extraction and recovery of paracetamol compound across different affinity polymer membranes . Parameters and mechanisms. *European Journal of Pharmaceutics and Biopharmaceutics*. Elsevier B.V.201–210. doi: https://doi.org/10.1016/j.ejpb.2017.06.001

Eljaddi T et al (2015) Effective supported liquid membranes for facilitated extraction phenomenon of cadmium (ii) ions from acidic environments: parameters and Mechanism. *Can J Chem Eng* 93:1–9. https://doi.org/10.1002/cjce.22144

Hao Z. *et al.* (2017) *2.14 Liquid Membranes*. 2nd edn.*Comprehensive Membrane Science and Engineering*. 2nd edn. Elsevier BV. https://doi.org/10.1016/b978-0-12-409547-2.12281-4

Hu X. Y. *et al.* (2019a) How much can we trust polysorbates as food protein stabilizers - the case of bovine casein. *Food Hydrocolloids*.81–92. https://doi.org/10.1016/j.foodhyd.2019.05.013

Hu Y. et al. (2019b) Occurrence, behavior and risk assessment of estrogens in surface water and sediments from Hanjiang River, Central China. Ecotoxicology. Elsevier Inc.143–153. https://doi.org/10.1007/s10646-018-2007-4

Kamal O et al (2017) Grafted polymer membranes with extractive agents for the extraction process of VO2+ ions. *Polym Adv Technol* 28:541–548. https://doi.org/10.1002/pat.3955

Kamrani M., Akbari A. and Yunessnia lehi A. (2018) Chitosan-modified acrylic nanofiltration membrane for efficient removal of pharmaceutical compounds. *Journal of Environmental Chemical Engineering*. Elsevier B.V.583–587. https://doi.org/10.1016/j.jece.2017.12.044

Lewis S. R. *et al.* (2012) Tunable separations, reactions, and nanoparticle synthesis in functionalized membranes. In *Responsive Membranes and Materials*. doi: https://doi.org/10.1002/9781118389553.ch5

Li C, Cabassud C, Guigui C (2015a) Evaluation of membrane bioreactor on removal of pharmaceutical micropollutants: a review. *Desalin Water Treat* 55:845–858. https://doi.org/10.1080/19443994.2014.926839

Li Y et al (2015b) Facilitated transport of small molecules and ions for energy-efficient membranes. *Chem Soc Rev* 44:103–118. https://doi.org/10.1039/c4cs00215f

Martinez J. L. (2009) Environmental pollution by antibiotics and by antibiotic resistance determinants. *Environmental Pollution*. Elsevier Ltd.2893–2902. https://doi.org/10.1016/j.envpol.2009.05.051

Sim W. J. *et al.* (2011) Occurrence and distribution of pharmaceuticals in wastewater from households, livestock farms, hospitals and pharmaceutical manufactures. *Chemosphere*. Elsevier Ltd.179–186. https://doi.org/10.1016/j.chemosphere.2010.10.026

Spas D. Kolev (2019) *Membrane Techniques: Liquid Membranes*. 3rd edn. *Encyclopedia of Analytical Science*. 3rd edn. Elsevier Inc https://doi.org/10.1016/B978-0-12-409547-2.14301-X

Taheran M. *et al.* (2016) Membrane processes for removal of pharmaceutically active compounds (PhACs) from water and wastewaters. *Science of the Total Environment*. Elsevier B.V.60–77. https://doi.org/10.1016/j.scitotenv.2015.12.139

C.J.M. van Rijn (2004) Chapter 1 Overview membrane technology.in *Membrane Science and Technology*. Elsevier BV.1–23. https://doi.org/10.1016/S0927-5193(04)80018-4

Wang G et al (2018) Removal of norfloxacin by surface Fenton system (MnFe2O4/H2O2): kinetics, mechanism and degradation pathway. *Chem Eng J* 351:747–755. https://doi.org/10.1016/j.cej.2018.06.033

Wang Z. *et al.* (2019) A fast strategy for profiling and identifying pharmaceutic excipient polysorbates by ultra-high performance liquid chromatography coupled with high-resolution mass spectrometry. *Journal of Chromatography A*. Elsevier B.V.460–450. https://doi.org/10.1016/j.chroma.2019.460450

Watson H (2015) Biological membranes. *Essays Biochem* 59:43–70. https://doi.org/10.1063/1.2913788

Xu Y, Chen C, Li J (2007) Experimental study on physical properties and pervaporation performances of polyimide membranes. *Chem Eng Sci* 62:2466–2473. https://doi.org/10.1016/j.ces.2007.01.019